J. Phys.: Condens. Matter **21** (2009) 045402 (7pp) doi:10.1088/0953-8984/21/4/045402

Solid-state amorphization of a quenched high-pressure GaSb phase studied by real-time neutron diffraction: evolution of the crystalline phase

V K Fedotov[1,4], O I Barkalov[1], E G Ponyatovsky[1], M Calvo-Dahlborg[2], U Dahlborg[2] and T Hansen[3]

[1] Institute of Solid State Physics RAS, 142432 Chernogolovka, Moscow District, Russia
[2] Groupe de Physique des Materiaux—UMR CNRS 6634 Institut des Materiaux, UFR Sciences et Techniques Avenue de l'Université, BP 12, F-76801 Saint-Etienne du Rouvray Cedex, France
[3] Institute Laue-Langevin, BP 156, F-38042 Grenoble Cedex 9, France

E-mail: fedotov@issp.ac.ru

Received 19 September 2008, in final form 20 November 2008
Published 19 December 2008
Online at stacks.iop.org/JPhysCM/21/045402

Abstract
The amorphization of a quenched sample of the GaSb-II high-pressure phase was studied at ambient pressure by real-time neutron diffraction in the course of the sample heating from 100 K to room temperature at a rate of 0.4 K min^{-1}. The transformation to the amorphous state begins at 140 K and is completed near room temperature. The β-Sn type structure was shown to represent only the mean lattice of the high-pressure GaSb-II phase. The superstructure of this phase widely varied with temperature and is caused by the ordered displacement of atoms. The temperature range of the metastable crystalline phase relaxation is divided into three intervals according to the temperature dependence of the tetragonality ratio (c/a). At the boundaries of these temperature intervals, i.e. temperatures $T = 170$ and 230 K, two second-order phase transitions are observed. Anomalous heat and volumetric effects were observed earlier by means of calorimetry and dilatometry in the same temperature range. Variation of the β-Sn type crystal structure reflects the general tendency of ideal tetrahedral bond network recovery. All phase transformations observed were found to be irreversible.

(Some figures in this article are in colour only in the electronic version)

1. Introduction

The low-pressure GaSb-I phase is a semiconductor with a site-ordered cubic crystal structure of the zinc-blende type. Under a hydrostatic pressure of 6–7 GPa and room temperature, the GaSb-I phase transforms to a metallic GaSb-II phase with a site-disordered tetragonal structure of the β-Sn type [1–3]. If the pressure is non-hydrostatic, a site-disordered orthorhombic phase with *Imma* symmetry is formed instead of the GaSb-I phase, and this *Imma* phase transforms to GaSb-II if heated to 473–500 K at a pressure from 7–13 GPa [2, 4] or to another site-disordered orthorhombic *Ammm* phase if heated to 473 K at a pressure above 20 GPa [4].

The GaSb-II phase can be retained at ambient pressure if previously quenched under high pressure to liquid nitrogen temperature. Further slow heating of this metastable phase to room temperature leads to its spontaneous amorphization [5, 6]. The process of the spontaneous amorphization of GaSb-II was studied by calorimetry and dilatometry. The measured dependences indicated the occurrence of three well-reproduced stages of amorphization substantially spaced apart in temperature [7–9]. The resulting amorphous phase, a-GaSb, is thermally stable at room temperature and irreversibly transforms to the crystalline

[4] Author to whom any correspondence should be addressed.

GaSb-I phase on heating to 470 K. The structure of a-GaSb was intensely studied by neutron diffraction [10–12] and x-rays [13, 14] and by EXAFS [15, 16] and was shown to be some amorphous analogue of the GaSb-I crystal structure. All studies demonstrated that the ideal tetrahedral arrangement of atoms characteristic of the GaSb-I structure is distorted in the amorphous phase. It was shown in [17] that a-GaSb phase is a semiconductor, though a rather unusual one, as its electrical properties can only be explained assuming that the Fermi level lies inside the valence band tail instead of being pinned within the mobility gap.

The process of spontaneous amorphization of the quenched GaSb-II phase extends over a wide temperature interval from about 100 K to room temperature, which provides a good opportunity for its detailed investigation. In the present paper, the evolution of the structure and the mole fraction of both GaSb-II and a-GaSb phases in the course of heating the quenched GaSb-II phase at ambient pressure was monitored by real-time neutron diffraction. The main target of the present investigation was to elucidate the relationship between the structural changes of the crystalline and amorphous phases and anomalous heat and volumetric effects observed upon amorphization and corresponding to the different stages of this process.

2. Sample preparation and experimental details

A sample of the GaSb-II high-pressure phase was prepared from a single crystal of GaSb-I crushed into powder in an agate mortar to avoid possible texture effects. The powder was pressed into pellets 7 mm in diameter and 2 mm thick and each pellet was individually placed in a Teflon container, exposed to a pressure of 7.0 GPa at 520 K for 24 h using a toroid-type high-pressure chamber, cooled to 100 K together with the chamber and, after the pressure was released, examined by x-ray diffraction at 90 K to ensure that it had completely transformed to the GaSb-II phase. The GaSb-II sample with a volume of about 0.5 cm^3 was assembled from eight such pellets. While at ambient pressure, the sample was never warmed above 100 K and it was transported and stored in liquid nitrogen prior to the neutron diffraction experiment.

The GaSb-II sample thus prepared was studied with the D20 diffractometer at the Institute Laue-Langevin in Grenoble in the course of heating from 100 K to room temperature at a rate of 0.4 K min^{-1} using neutrons of a wavelength of $\lambda = 2.4215$ Å. Stacked pellets were enclosed in a cylindrical, thin-walled vanadium can and placed in a continuous-flow helium 'orange' cryostat. The background was determined in a separate empty-can measurement and subtracted from the measured diffraction patterns. The diffraction data for the crystalline phase were analysed using a computer program [18] based on the Rietveld profile refinement technique.

The amorphization of the GaSb-II phase is a non-equilibrium process accompanied by a significant heat emission of (3.5 ± 0.5) kJ mol^{-1} [9] and, in the absence of an efficient thermal stabilization, the resulting self-heating leads to a sudden complete amorphization immediately followed by the complete crystallization, because the crystallization of a-GaSb is also a non-equilibrium process with a heat release of (8.3 ± 1) kJ mol^{-1} [9]. For example, using nitrogen as the purge gas and the heating rate of 1 K min^{-1} resulted in a premature explosion-like crystallization of the quenched GaSb-II sample when we tried to study its amorphization process by real-time neutron diffraction for the first time [19]. The better heat exchange between the sample and helium gas in the 'orange' cryostat together with the low heating rate of 0.4 K min^{-1} in the present experiment efficiently prevented the sudden crystallization of the sample.

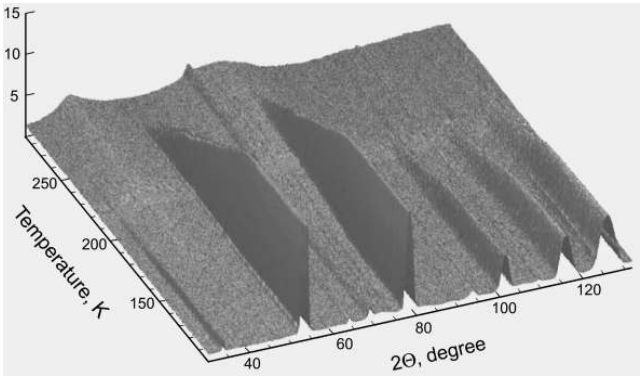

Figure 1. Neutron powder diffraction patterns demonstrating the process of spontaneous amorphization of a quenched GaSb-II sample in the course of its heating at ambient pressure at a rate of 0.4 K min^{-1}. The patterns are measured with the D20 diffractometer at ILL, Grenoble in a 'real-time' regime using neutrons of a wavelength of $\lambda = 2.4215$ Å. The last snapshot taken at room temperature shows diffraction haloes of the amorphous a-GaSb phase superimposed on two diffraction lines from the vanadium can ($2\theta = 70°$ and 110°).

3. Results

Figure 1 presents an overview of the whole set of diffraction patterns measured during the slow heating of the quenched sample of the GaSb-II high-pressure phase. Starting from about 140 K, the intensity of diffraction lines of the crystalline GaSb-II phase gradually decreases until the lines vanish completely at about 260 K. The decrease in the intensity of the GaSb-II lines is followed by a gradual increase in the intensity of diffuse neutron scattering and the patterns measured at temperatures exceeding 260 K are characteristic of the amorphous phase.

3.1. Evolution of the crystalline metallic GaSb-II phase

Figure 2 illustrates characteristic features of diffraction patterns of the GaSb sample and their evolution with increasing temperature. As one can see, every main line of the starting metastable high-pressure phase GaSb-II at $T = 100$ K is well modelled with the β-Sn type structure, while the $Imma$ structure is qualitatively inapplicable. This agrees with the observation of [2, 4] that the high-pressure low-temperature $Imma$ phase of GaSb irreversibly transforms to the β-Sn type GaSb-II phase if heated to 473–500 K at a pressure from

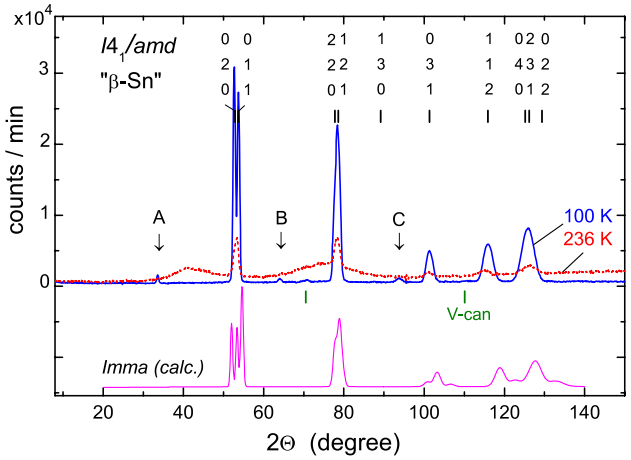

Figure 2. Experimental neutron diffraction patterns of the GaSb sample measured at 100 and 236 K and the calculated profile for the high-pressure *Imma* structure of GaSb suggested in [4]. The main peaks in the experimental patterns are indexed with a tetragonal unit cell of the β-Sn type (space group $I4_1/amd$) and three additional weak peaks are marked with downward arrows. Two vertical bars beneath the experimental patterns show the positions of diffraction peaks from the vanadium can.

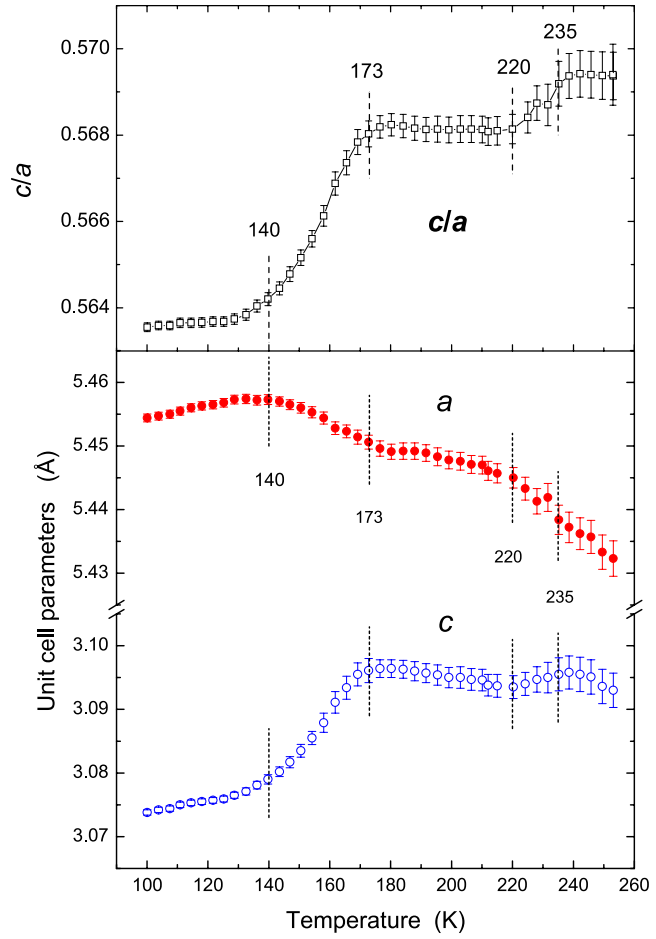

Figure 3. Temperature dependences of the lattice parameters, a and c, and the tetragonality ratio c/a of the GaSb-II phase in the quenched GaSb sample heated at 0.4 K min^{-1}. The increase in the experimental errors at increasing temperature is due to the decrease in the fraction of this phase in the GaSb-II/a-GaSb mixture.

7–13 GPa, because the high-pressure phase was formed at 7.0 GPa at 520 K in the present work. The refined values of the lattice parameters of the tetragonal β-Sn type structure (space group $I4_1/amd$) of the GaSb-II phase at 100 K were $a = 5.4544(5)$ Å and $c = 3.0738(4)$ Å, which corresponded to the ratio of $c/a = 0.563\,55(9)$ and the atomic volume $V_a = a^2c/4 = 22.862(2)$ Å^3/atom.

The effect of slow heating from 100 K to room temperature on the lattice parameters, c/a ratio and volume of the tetragonal unit cell of the GaSb-II phase is shown in figures 3 and 4. Figure 5(a) presents the relative intensities of three weak diffraction lines of this phase marked with vertical arrows and the letters A, B and C in figure 2. Figure 5(b) demonstrates the variation of the mole fractions P_i, of the GaSb-II and a-GaSb phases in the heated sample.

There are three weak lines—A, B and C—in the diffraction pattern of the GaSb-II phase shown in figure 2 that cannot belong to the lines of a site-disordered β-Sn type structure. Similar weak lines were earlier observed in x-ray [3, 4] and neutron [11] diffraction patterns of this phase, but they were tentatively attributed to the presence of a new and unidentified minority high-pressure high-temperature phase. We think these lines pertained to the GaSb-II phase because in our experiment their intensity decreased with increasing temperature approximately in direct proportion to the intensity of the main lines of this gradually disappearing phase (see figure 5(a)). Superstructural lines A, B and C in figure 2 can be indexed as reflections (111), (013) and (133) of a cubic cell with the lattice parameter $a = 7.23(1)$ Å and $N \approx 16$ atoms in the unit cell.

Most likely, the weak additional lines are due to a displacive ordering in the site-disordered β-Sn type crystal lattice of the GaSb-II phase. The displacive character of the superstructure follows from the fact that the relative intensities of these lines in the x-ray [4] and neutron diffraction patterns (figure 2) proved to be approximately the same, while the site ordering would have resulted in the threefold difference due to the difference in the x-ray and neutron scattering amplitudes of the Ga and Sb atoms. The ordering in the β-Sn type mean lattice of the GaSb-II phase is obviously too complex to be determined using a polycrystalline sample. Nevertheless, this ordering proved to exert a noticeable influence upon the parameters of the mean lattice, as their temperature dependences showed anomalies that could be attributed only to significant changes in the superstructure.

The behaviour of the a, c and c/a dependences (figure 3) suggests that the investigated temperature range 100–282 K can be divided into five intervals with boundaries at approximately 140, 173, 220 and 235 K shown by vertical dashed lines. At temperatures up to 140 K, both a and c increase with temperature, demonstrating the thermal expansion typical of most metallic phases. At 140 K, the a parameter reaches its maximum and starts decreasing. The increase in c continues and even accelerates until it abruptly stops at around 170 K, and the c parameter starts decreasing, so that the c/a ratio remains virtually constant at temperatures

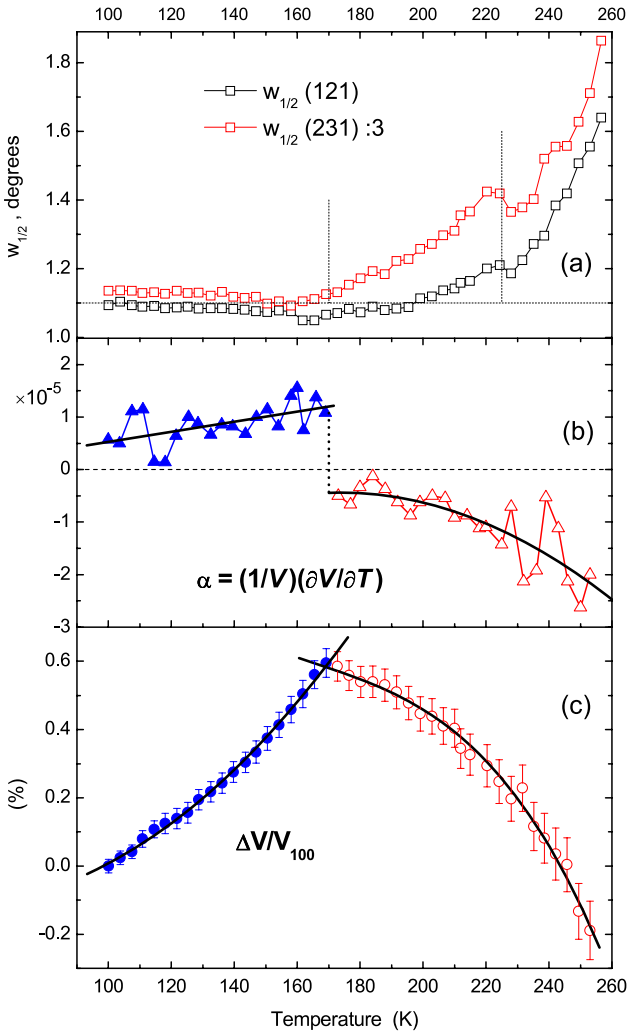

Figure 4. The half-width of the Bragg peaks (121) and (231) calculated by profile analysis method (a), the coefficient α of volume expansion (b) and the relative increment $\Delta V/V_{100\ \mathrm{K}}$ of the volume of the β-Sn type unit cell of the GaSb-II phase in the quenched GaSb sample heated at 0.4 K min^{-1} (c).

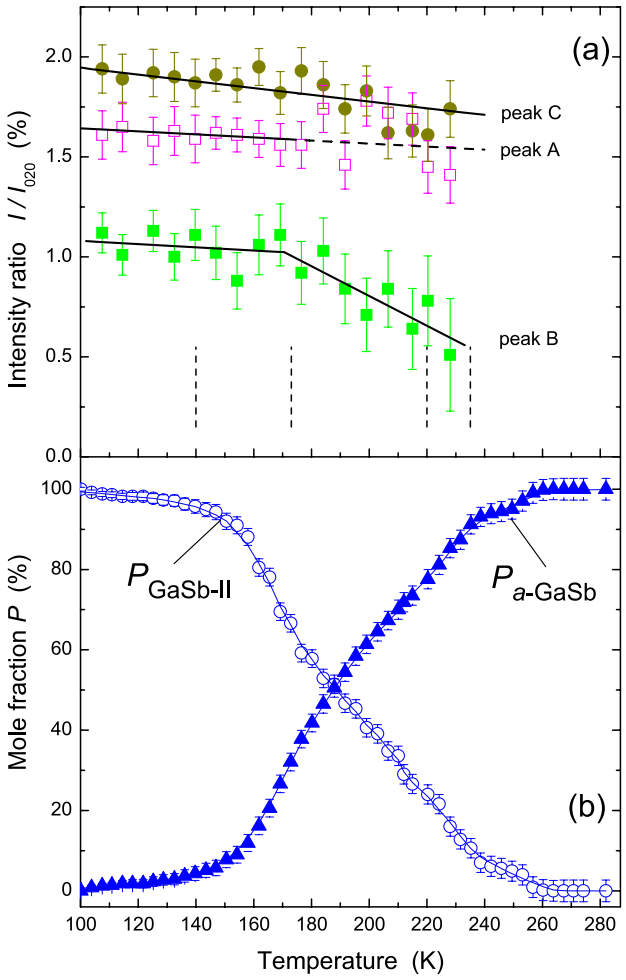

Figure 5. (a) The ratios of the integral intensities of superstructural diffraction lines A, B and C to the intensity of the (020) line of the β-Sn type mean lattice of the GaSb-II phase (see the pattern labelled 100 K in figure 2). (b) The variation of the mole fractions, P, of the GaSb-II and a-GaSb phases on heating the quenched GaSb-II sample at a rate of 0.4 K min^{-1}. The fractions were calculated based on the profile analysis of the diffraction patterns of the crystalline GaSb-II phase (open circles) and the integral intensity scattered by the amorphous a-GaSb phase (solid triangles). Where the fraction of the given phase was small, it was determined as 100% $-P$ using the calculated fraction P of another phase.

between 170 and 220 K. The c/a ratio increases again on heating from about 220 to 235 K and stops varying at higher temperatures.

The temperature dependence of the volume of the GaSb-II phase exhibits no anomalies at 140 and 220–235 K, but it shows a maximum exactly at 170 K (figure 4(c)). As one can see from the solid lines of polynomial fits, the $V(T)$ curve is concave at temperatures below 170 K and convex at higher temperatures. The coefficient α of volume expansion (figure 4(b)) therefore changes from positive to negative magnitudes in a jump-like manner characteristic of second-order phase transitions. The discontinuous jump of α is clearly seen from the differentiated smooth curves used to fit the experimental $V(T)$ dependence (that is the common practice to reveal such discontinuities). Moreover, the jump is large enough to be seen even from the numerically differentiated experimental $V(T)$ data (points connected by thin solid lines in figure 4(c)), despite their scatter. This leaves no doubts as to the occurrence of a second-order phase transition in the GaSb-II phase at 170 K. To emphasize the presence of superstructures with different symmetries, we showed the data points in figure 4 using different symbols, open and solid, at temperatures below and above 170 K, respectively.

It seems worth noting that, despite the absence of noticeable anomalies in the $V(T)$ dependence at 220–235 K, the stepwise increase in the c/a ratio inside this temperature interval is rather indicative of another second-order phase transition, since one should expect a monotonic variation of structure parameters of any phase within the temperature range of its stability. Interestingly, the phase transition at 170 K does not much affect the relative intensities of the three superstructural diffraction lines (figure 5(a)). A change in the slope might only occur in the intensity dependence of line B at this temperature (see the solid line), but the dependence might be smooth as well within the experimental

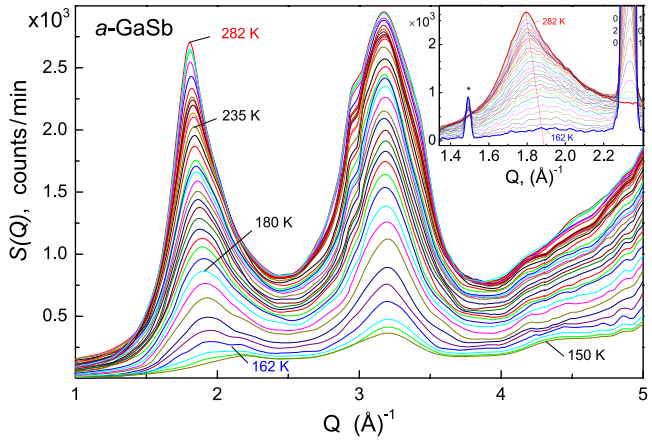

Figure 6. Spectra of diffuse neutron scattering from the quenched GaSb sample heated at 0.4 K min^{-1}. To calculate these spectra, groups of every ten successive snapshots shown in figure 1 were merged to achieve better statistical accuracy (the result is illustrated by the inset) and then the contribution from the crystalline GaSb-II phase was evaluated and subtracted.

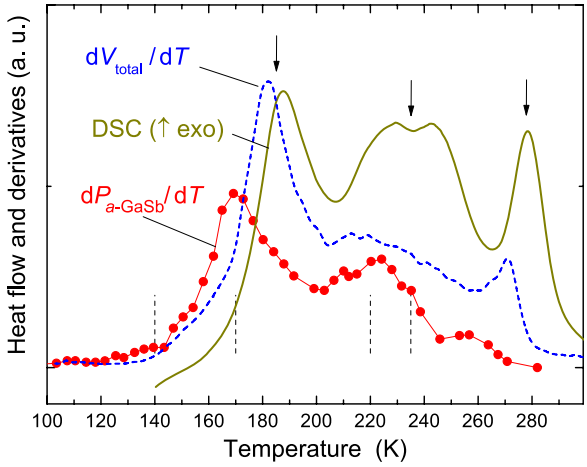

Figure 7. Temperature dependences of the heat flow (DSC curve, 5 K min^{-1}) [8] and the first derivatives with respect to temperature of the total volume ($\mathrm{d}V_{\mathrm{total}}/\mathrm{d}T$ curve, 5 K min^{-1}) [8] and the mole fraction of the amorphous phase ($\mathrm{d}P_{\mathrm{a\text{-}GaSb}}/\mathrm{d}T$ curve, 0.4 K min^{-1}) during the heating of a quenched sample of the GaSb-II phase. The solid curve that fits the $\mathrm{d}P_{\mathrm{a\text{-}GaSb}}/\mathrm{d}T$ dependence is the derivative of the solid curve fitting the $P_{\mathrm{a\text{-}GaSb}}(T)$ dependence in figure 5(b). Vertical dashed lines are given at the positions as in figure 3 for comparison (see the text). Downward arrows designate approximate positions of the peaks on the DSC and $\mathrm{d}V_{\mathrm{total}}/\mathrm{d}T$ curves discussed in the text.

error. The steep increase in the c/a ratio of the GaSb-II phase at temperatures approaching 170 and in the interval 220–235 K can be related to the degree of conversion of GaSb-II to a-GaSb that demonstrates the steepest temperature dependence at these very temperatures (figure 5(b)).

3.2. Evolution of the amorphous semiconductor a-GaSb

As seen from figure 5(b), the a-GaSb phase starts intensely growing at approximately 120–140 K. Two broad diffuse peaks characteristic of a-GaSb (see the curve labelled '236 K' in figure 2) can be reliably distinguished from the background of neutron diffraction patterns already at 160 K. However, these peaks are superimposed onto intense diffraction lines of the crystalline GaSb-II phase that coexists with a-GaSb at temperatures up to approximately 260 K (figure 1). To isolate the diffuse neutron scattering resulting from a-GaSb in the two-phase mixtures, groups of every ten successive snapshots shown in figure 1 were first merged to achieve better statistical accuracy. The diffraction patterns obtained in this way in the range of the first diffuse peak are shown in the inset to figure 6. The contribution from the crystalline GaSb-II phase to each of these patterns was then evaluated by profile analysis and subtracted. The resulting spectra of diffuse neutron scattering from the a-GaSb phase are shown in figure 6 as functions of the momentum transfer $Q = (4\pi/\lambda)\sin\theta$.

In order to check the reversibility of the structural changes occurring in the course of the amorphization process, heating of the sample was stopped once somewhere in the middle of the transformation temperature range at 212 K and then close to the end of it, at 282 K. The sample was cooled down to 205 and 103 K, respectively. The diffraction patterns of the sample at high and low temperatures, if the thermal factor was taken into account, were found to be identical. This indicates that the transformations occurring upon heating are irreversible.

4. Discussion

The multistage character of the amorphization process is well seen in figure 7 from the temperature dependence $\mathrm{d}P_{\mathrm{a\text{-}GaSb}}/\mathrm{d}T$ of the rate of the GaSb-II to a-GaSb conversion constructed in this work and also from the DSC trace and $\mathrm{d}V_{\mathrm{total}}/\mathrm{d}T$ curve measured earlier [8] on heating at 5 K min^{-1}. The latter two dependences look similar and show three broad peaks at around 185, 230 and 275 K, indicated by vertical arrows. Of these dependences, the $\mathrm{d}V_{\mathrm{total}}/\mathrm{d}T$ curve should more accurately represent the growing fraction $P_{\mathrm{a\text{-}GaSb}}$ of the a-GaSb phase, because the transformation of the dense metallic GaSb-II phase to the semiconductor a-GaSb phase is accompanied by a large volume increase of approximately 24% [9] that significantly exceeds the small changes in the atomic volume of the GaSb-II phase (figure 4(c)).

As seen from figure 7, there are two distinct peaks at 170 and 225 K in the $\mathrm{d}P_{\mathrm{a\text{-}GaSb}}/\mathrm{d}T$ curve constructed in the present work. The shapes and positions of these peaks significantly differ from those of peaks of the $\mathrm{d}V_{\mathrm{total}}/\mathrm{d}T$ curve, most likely because of the much lower rate of 0.4 K min^{-1} of the sample heating. Nevertheless, the peak at 170 K can unambiguously be related to the 186 K peak in the $\mathrm{d}V_{\mathrm{total}}/\mathrm{d}T$ curve. The high-temperature shoulder of the 225 K peak in the $\mathrm{d}P_{\mathrm{a\text{-}GaSb}}/\mathrm{d}T$ curve and the 278 K peak in the $\mathrm{d}V_{\mathrm{total}}/\mathrm{d}T$ curve should rather be of the same origin as they both characterize the formation of the last 10% of the amorphous phase. The process giving rise to the peak at 225 K in the $\mathrm{d}P_{\mathrm{a\text{-}GaSb}}/\mathrm{d}T$ dependence should therefore also contribute to the broad peak centred at 230 K in the $\mathrm{d}V_{\mathrm{total}}/\mathrm{d}T$ dependence.

As for the factors that determine the amorphization rate, their full analysis is a rather difficult problem, first

of all, because of the ill-controlled effects of the strong and inhomogeneous stress field arising in the sample due to the large difference in the atomic volumes of the GaSb-II and a-GaSb phases. A notable feature of the solid-state amorphization of GaSb-II is that the resulting amorphous sample maintains its integrity and does not crack [8]. In view of the large volume increase of about 24% accompanying the amorphization [9], the integrity of the sample necessitates the occurrence of macroscopic fluxes of the material of both GaSb-II and a-GaSb phases. Generation of such fluxes requires elastic forces of the order of the yield limit of these phases, if there is no alternative route for the relaxation of these strains.

By the value of Bragg peak dispersion one can monitor the reaction of the crystalline matrix on amorphization process and control the fields of elastic stresses (figure 4(a)). In this case the general increase with temperature of the half-width of the marked reflections can be attributed to the decrease of the grain size, while the relative half-width increase of the remote peak (231) is due to lattice distortions. The effects observed are of medium range order or even of minimum one (for temperatures below 170 K), but not enormous effects that one can expect, taking into account the volume effect of amorphization, i.e. about 24%.

The diffraction method used here is of low sensitivity to the ordering of the GaSb alloy. This is due to the small difference of the scattering amplitudes of neutrons for the alloy components. Therefore, the GaSb-I (type ZnS) $\leftrightarrow$ GaSb-II transition appears to be analogous to the α-Sn $\leftrightarrow$ β-Sn transition: the scheme of the latter was proposed in [20]. The cubic structure of α-Sn can also be regarded as a body-centred structure having a particular value of the axial ratio of $c/a = \sqrt{2}$ that gives rise to the higher cubic symmetry. The β-Sn structure can be transformed to α-Sn by a continuous increase in the c/a ratio from 0.544 to $\sqrt{2}$. This leads to the decrease in the coordination numbers from $(4+2)+4+8$ for β-Sn to $4+12$ for α-Sn and to the concomitant 21.3% increase in the atomic volume.

Certainly, the character of so significant changes of the crystalline structure cannot be continuous. One should rather expect sudden cooperative transformations based on the translational symmetry and preconditioned by the stress fields in the high-pressure cell. Several mechanisms of the transformation can be proposed with a number of intermediate states that can be fixed as metastable phases. The large total volume effect has to be separated within the interval of transformation and should be remarkable. But in our case the relative change of high-pressure phase volume does not exceed 0.6% (figure 4(c)). Nevertheless, analysis of the tetragonal cell lattice parameters (figure 3) reveals that the general tendency of metal-to-semiconductor transition persists as a recovering of the destroyed tetragonal bonds. This effect is the most prominent in the 140–180 K temperature interval. This manifests itself by a small decrease in the tetrahedron angle $\alpha_T = 2\,\mathrm{arcctg}(c/2a)$ and shortening of the bond lengths in the first coordination sphere.

Then, at the temperatures above 180 K amorphous phase fraction surpasses 50% (figure 5(b)) and the above-mentioned tendency declines, most probably due to the transitions in the surrounding amorphous medium. In this case the elastic stresses may govern the lattice parameter behaviour and result in a decreasing of amorphization rate (figure 7). On the other hand, when the fraction of the amorphous phase is large enough the connectivity of the crystalline metallic grains will be broken, thus resulting in a significant decrease of the sample thermal conductivity. This, in its turn, causes local overheating and subsequent acceleration of the amorphization process at temperatures above 210 K, judging from the relevant singularities of the curves in figures 3, 4 and the appearance of the second heat release peak in figure 7.

Recovery of the tetrahedral coordination within the crystalline high-pressure phase is of continuous and gradual character in contrast to the formation of the amorphous phase. In the latter case spasmodic changes of the short range order take place, resulting in formation of the covalent bonds. Thus, we consider the final state of the amorphization process attained at room temperature as an unaccomplished stage of the ideal tetrahedral coordination recovering process. According to our previous neutron diffraction study the first coordination number is $n_1 > 4$, the length of the unsaturated bond $r_1 = 2.66$ Å > 2.64 Å and the bond angle is close to the ideal tetrahedral one [10, 11].

5. Conclusions

This has been the first structural investigation of solid-state amorphization of a high-pressure phase and we chose GaSb as the simplest object with the coinciding equiatomic composition of the high-pressure and low-pressure phases, the simple site-disordered β-Sn type structure of the high-pressure phase and the same tetrahedral arrangement of atoms in the amorphous phase and in the cubic zinc-blende type structure of the low-pressure phase. Nevertheless, the structures of the vanishing high-pressure phase and growing amorphous phase both demonstrated a rather complex behaviour with increasing temperature.

The β-Sn type structure was shown to represent only the mean lattice of the high-pressure GaSb-II phase. The superstructure of this phase is, in general, a displacement superstructure and it is not linked to the basis of the mean lattice by any simple relationship. Nevertheless, some weakening of the superstructure lines synchronous to that of matrix lines was observed in the course of increasing temperature.

The process of solid-state amorphization of the GaSb alloy is accompanied by anomalous structural changes of the initial crystalline phase proceeded in very much the same temperature intervals where peculiarities of heat release and sample expansion were observed earlier by calorimetry and dilatometry.

Variation of the lattice parameters of the crystalline phase follows the common tendency of the reverse transformation of β-Sn $\rightarrow$ α-Sn type and corresponds to the process of broken tetrahedral bonds recovering. This manifests itself by small decrease in the tetrahedron angle and shortening of the bond lengths in the first coordination sphere.

All structural transformations of the GaSb-II were irreversible and the structure of the amorphous sample heated to room temperature did not change back on further cooling. Absence of the large residual stresses in the crystalline matrix is the case for the plastic flow of the coexisting phases in the course of amorphization. This might explain why the continuity of the sample is retained despite the large volume effect of the amorphization, 24%.

Judging by the results for GaSb, structural investigation of the process of solid-state amorphization of high-pressure phases represents an efficient tool for studying the evolution of the structure of metastable phases down to low temperatures that cannot be achieved by other means.

Acknowledgments

This work was supported by the Programme 'Thermophysics and Mechanics of the Extreme Effects' of the Russian Academy of Sciences and by grant no. 07-02-00024 from the Russian Foundation for Basic Research.

References

[1] Minomura S and Drickamer H G 1962 *J. Phys. Chem. Solids* **23** 451
[2] Mezouar M, Libotte H, Deputier S, LeBihan T and Hauserman D 1999 *Phys. Status Solidi* b **211** 395
[3] Vanpeteghem C B, Nelmes R J, Allan D R, MacMahon M I, Sapelkin A V and Bayliss S C 2001 *Phys. Status Solidi* b **223** 405
[4] Vanpeteghem C B, Nelmes R J, Allan D R and McMahon M I 2001 *Phys. Rev.* B **65** 012105
[5] McDonald T R R, Sard R and Gregory E 1965 *J. Appl. Phys.* **36** 1498
[6] Degtyareva V F, Belash I T, Ponyatovsky E G and Raschupkin V I 1990 *Fiz. Tverd. Tela.* **32** 1429 (in Russian)
Degtyareva V F, Belash I T, Ponyatovsky E G and Raschupkin V I 1990 *Sov. Phys.—Solid State* **32** 834
[7] Ponyatovsky E G and Barkalov O I 1991 *Mater. Sci. Eng.* A **133** 726
[8] Barkalov O I, Ponyatovsky E G and Antonov V E 1993 *J. Non-Cryst. Solids* **156–158** 544
[9] Antonov V E, Barkalov O I and Ponyatovsky E G 1995 *J. Non-Cryst. Solids* **192/193** 443
[10] Barkalov O I, Kolesnikov A I, Antonov V E, Ponyatovsky E G, Dahlborg U, Dahlborg M and Hannon A 1996 *Phys. Status Solidi* b **198** 491
[11] Calvo-Dahlborg M, Dahlborg U, Barkalov O I, Kolesnikov A I, Ponyatovsky E G and Hannon A C 1999 *J. Non-Cryst. Solids* **244** 250
[12] Kolesnikov A I, Barkalov O I, Calvo-Dahlborg M, Dahlborg U, Howells W S and Ponyatovsky E G 2000 *Phys. Rev.* B **62** 9372
[13] Brazhkin V V, Lyapin A G, Khvostansev L G, Sidorov V A, Tsiok O B, Bayliss S C, Sapelkin A V and Clark S M 1996 *Phys. Rev.* B **54** 1808
[14] Demishev S V, Kosichkin Yu V, Lyapin A G, Sluchanko N E and Sharambeyan M S 1993 *Zh. Eksp. Teor. Fiz.* **104** 2388 (in Russian)
Demishev S V, Kosichkin Yu V, Lyapin A G, Sluchanko N E and Sharambeyan M S 1993 *Sov. Phys. —JETP* **77** 68
[15] Lyapin A G, Brazhkin V V, Bayliss S C, Sapelkin A V, Itie J P, Polian A and Clark S M 1996 *Phys. Rev.* B **54** 14242
[16] Sapelkin A V, Bayliss S C, Lyapin A G, Brazhkin V V and Dent A 1997 *Phys. Rev.* B **56** 11531
[17] Antonov V E, Barkalov O I, Kolyubakin A I and Ponyatovsky E G 1996 *Phys. Status Solidi* b **198** 497
[18] Young R A, Sakthivel A, Moss T S and Paiva-Santos C O 1995 *DBWS9411 User's Guide* (Atlanta: Georgia Institute of Technology) p 60
[19] Barkalov O I, Fedotov V K, Beskrovnyy A I and Petrov M Ju 1999 *Poverkhnost'. Rentgenovskie, Sinkhrotronnye i Neitronnye Issledovaniya* **2** 10 (in Russian)
[20] Musgrave J P 1963 *Proc. R. Soc.* **272** 503